26 May 2010, 4:45 pm - 6:45 pm

Correlation Between Low Strain Shear Modulus and Standard Penetration Test 'N' Values

P. Anbazhagan
Indian Institute of Science, India

T. G. Sitharam
Indian Institute of Science, India

P. Aditya
Indian Institute of Science, India

Fifth International Conference on
Recent Advances in Geotechnical Earthquake Engineering and Soil Dynamics
and Symposium in Honor of Professor I.M. Idriss
May 24-29, 2010 • San Diego, California

CORRELATION BETWEEN LOW STRAIN SHEAR MODULUS AND STANDARD PENETRATION TEST 'N' VALUES

Anbazhagan, P
Department of Civil Engineering,
Indian Institute of Science, Bangalore, India 56001

Sitharam, T. G and Aditya, P.
Department of Civil Engineering,
Indian Institute of Science, Bangalore, India 56001

ABSTRACT

In this study an attempt has been made to develop correlation between standard penetration test (SPT) N values and low strain shear modulus (G_{max}). The field experiments of Multichannel Analysis of Surface Wave (MASW) are carried out at 38 locations close to boreholes having Standard Penetration Test N values and in-situ density. These experimental data were generated and used for seismic microzonation of Bangalore, India. In-situ densities of subsurface layers were obtained from undisturbed soil samples collected from the boreholes. Shear wave velocity (Vs) profile with depth were obtained for the same locations or close to the boreholes using MASW. The low strain shear modulus values have been calculated using measured Vs and soil density. About 215 pairs of SPT N and shear modulus values are used for regression analysis and correlation between them are developed. The differences between fitted regression relations using measured and corrected N values were analyzed and presented. More details of correlation between shear modulus versus measured and corrected SPT N values and comparisons are presented elsewhere.

INTRODUCTION

The dynamic properties in terms of shear wave velocity with density or shear modulus are the most important properties to model the seismic wave propagation. These are used to understand and predict the source, path and site effects due to earthquake/similar type of loading system. Shear wave velocity of subsurface is the widely used parameter in site response and seismic microzonation. Site amplification of seismic energy due to local soil conditions and damage to built environment were amply demonstrated by many earthquakes during the last century (Guerrero earthquake (1985) in Mexico city, Spitak earthquake (1988) in Leninakan, Loma Prieta earthquake (1989) in San Francisco Bay area, Kobe earthquake (1995) in Japan, Kocaeli earthquake (1999) in Turkey and Bhuj earthquake (2001) in India). The recent 2001 Gujarat-Bhuj earthquake in India is another example, with notable damage at a distance of 250 km from the epicenter. These failures are due to effects of local soil conditions on the ground motion that are translated to higher amplitude (Anbazhagan and Sitharam, 2008a). The amount of modification of the spectral content and duration of ground motions are directly related to the variation of dynamic properties of layers. The response of a local site depends upon the frequency of the base motion and the geometry and dynamic properties of the soil layers above the bedrock. seismic microzonation considering geotechnical aspects requires shear wave velocity and shear modulus as input to estimate site specific ground response parameters (Sitharam and Anbazhagan, 2008a; Anbazhagan et al., 2009a). The site specific ground response studies needs input soil parameters, such as the thickness (h), density (ρ), and shear modulus (G_{max}) for each layer. The soil type and thickness of each layer are generally obtained by drilling boreholes and logging the borehole information (borelog). The in-situ densities of each layer are usually obtained from undisturbed soil samples collected in boreholes. In most cases, the shear modulus (G_{max}) for site response analysis is evaluated using relationships based on the SPT N values. These relationships are region specific, which depends on the type and characteristics of the soil in that region. It is not always fair to use existing correlations to obtain shear modulus for ground response study if soil conditions are not similar. This paper presents the relationship between SPT N value and G_{max} developed by authors for the residual soil found in Bangalore, India.

The low strain shear modulus (G_{max}) was evaluated using measured shear wave velocity obtained from MASW system and in-situ density from undisturbed soil samples obtained at the same depth in the corresponding boreholes. These values are used to generate a correlation between SPT measured and corrected 'N' values and G_{max}. This paper presents the summary of total work by authors and more details about the developed relationships that are available in Anbazhagan and Sitharam (2010).

STUDY AREA

The experiments are carried out in the Bangalore metropolitan area (Bangalore Mahanagar Palike), having an area of 220 km^2. Bangalore is situated on latitude 12^o 58' North and longitude 77^o 36' East and is at an average altitude of around 910 m above mean sea level (MSL). The basic geomorphology of the city comprises of a central Denudational Plateau and Pediment (towards the west) with flat valleys that are formed by the present drainage patterns. The central Denudational Plateau is almost void of any topology and the erosion and transportation of sediments carried by the drainage network gives rise to lateritic clayey alluvium seen throughout the central area of the city. This soil is mainly a product of strong weathering, ferruginous, clay mixture and well drained. The main types of soils found here are Red alluvium, sandy silts, alluvial clays, weathered rock (gravels), and soil fill material. The soil fill materials are a mixture of loose soil (excavated from constructions sites) and stones or building construction waste. Red alluvium (Lateritie) tropical residual soil is formed due to the erosion of the granitic and gneissic base rocks and this alluvium is ferruginous and is generally encountered in a clayey matrix. The erosion was caused by the natural drainage grid of lakes and streams throughout the city. Weathered rocks are generally granitic in composition and weathered from the parent rock and eventually combine with the sandy/clayey matrix. The locations of the field testing points for both borehole and MASW survey in Bangalore are shown in Fig. 1. The test locations were selected in such a way that these represent the entire city subsurface information. In total 38 one-dimensional (1-D) MASW surveys and 38 boreholes data have been used.

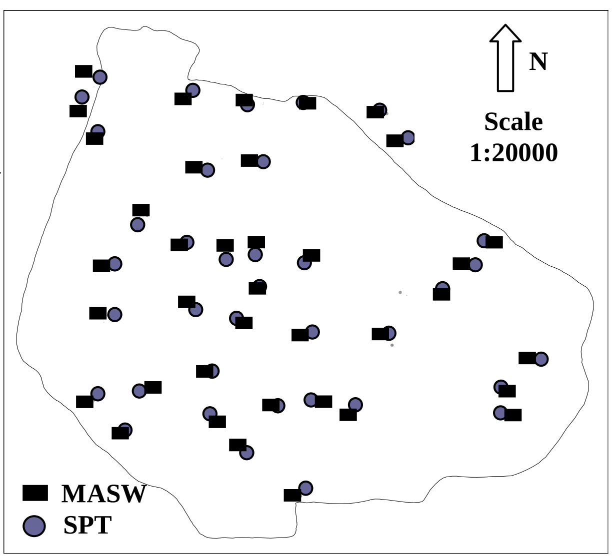

Fig. 1. MASW and SPT locations in the study area

SHEAR WAVE VELOCITY

A Multi-channel Analysis of Surface Wave (MASW) is a seismic refraction method, widely used for sub-surface characterization. MASW is increasingly being applied to earthquake geotechnical engineering for seismic microzonation and site response studies (Anbazhagan and Sitharam, 2008b). It can also be used for the geotechnical characterisation of near surface materials (Park et al, 1999; Xia et al, 1999; Miller et al, 1999; Kanli et al, 2006; Anbazhagan and Sitharam, 2008c). In particular, MASW is used in geotechnical engineering to measure the shear wave velocity and dynamic properties (Sitharam and Anbazhagan 2008b). It was used to identify the sub-surface material boundaries, spatial and depth variations of weathered and engineering rocks (Anbazhagan and Sitharam 2009a). Application of MASW is also extended in the railway engineering to identify the degree of fouling and type of fouling by Anbazhagan et al., (2009b). MASW generates a shear-wave velocity (Vs) profile (i.e., Vs versus depth) by analyzing Raleigh-type surface waves recorded on a multichannel. A MASW system consisting of 24 channels Geode seismograph with 24 vertical geophones of 4.5 Hz capacity have been used in this investigation. The seismic waves are created by an impulsive source of 15 pound (sledge hammer) with 300mmx300mm size hammer plate with number of shots. The optimum field parameters such as source to first and last receiver, receiver spacing and spread length of survey lines are selected in such a way that required depth of information can be obtained. These field parameters are in conformity with the recommendations of Park et al. (2002).

The captured seismic waves through geophones are recorded for duration of 1000 milli seconds. The quality of the recorded data is verified in the field itself. Noisy records are rerecorded to get better signals of record (Anbazhagan and Sitharam 2010). Typical recorded surface wave arrivals for a source to first receiver distance of 5m and processed data are shown in Fig. 2. These recorded data are further used to get dispersion curves, which are used to extract shear wave velocity at the midpoint of the testing locations. The shorter wavelengths are sensitive to the physical properties of surface layers (Xia et al., 1999). For this reason, a particular mode of surface wave will possess a unique phase velocity for each unique wavelength, leading to the dispersion of the seismic signal. For a multi layered subsurface model, Rayleigh-wave dispersion curves can be calculated by Knopoff's method (Schwab and Knopoff, 1972). Rayleigh-wave phase velocity, c_{Rj}, is determined by a characteristic equation F in its nonlinear, implicit form:

$$F(f_j, c_{Rj}, v_s, v_p, \rho, h) = 0 \quad (j = 1,2,......., m) \qquad (1)$$

where f_j is the frequency, in Hz; c_{Rj} is the Rayleigh-wave phase velocity at frequency f_j; $\mathbf{v}_s = (v_{s1}, v_{s2}, \ldots, v_{sn})^T$ is the S-wave velocity vector, with v_{si} the shear-wave velocity of the i^{th} layer; n is the number of layers; $\mathbf{v}_p = (v_{p1}, v_{p2}, \ldots, v_{pn})^T$ is the compressional P-wave velocity vector, with v_{pi} the P-wave velocity of the i^{th} layer; $\boldsymbol{\rho}=(\rho 1, \rho 2, \ldots, \rho n)^T$ is the density vector, with ρ_i the density of the i^{th} layer; and $\mathbf{h}=(h_1, h_2, \ldots, h_{n-1})^T$ is the thickness vector, with hi the thickness of the i^{th} layer. Given a set of model parameters (v_s , v_p, ρ, and h) and a specific frequency (f_j), the roots of equation (1) are the phase velocities. If the dispersion curve consists of m data points, a set of m equations in the form of equation (1) can be used to find phase velocities at frequencies f_j (j =1, 2, . . . ,m) using the bisection method (Press et al., 1992; Xia et al., 1999). In this study, only the fundamental mode is considered. The lowest analyzable frequency in this dispersion curve is around 4 Hz and highest frequency is 75Hz. A typical dispersion curve along with signal amplitude and signal to noise ratio is shown in Fig. 3. Each dispersion curve is generated for corresponding signal to noise ratio of about 80 and above.

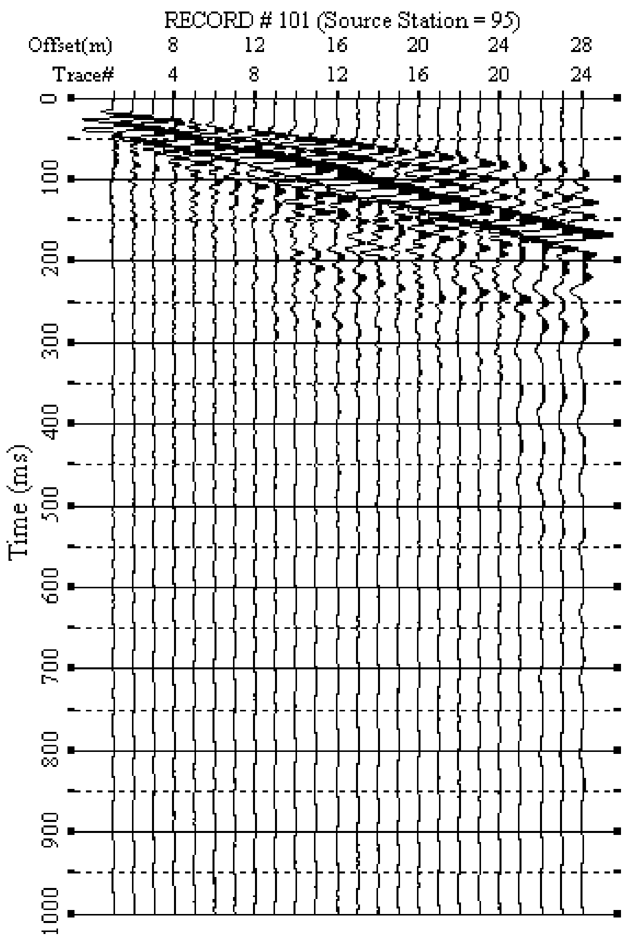

Fig. 2. Typical seismic data recorded during MASW survey

Shear wave velocity can be derived from inverting the dispersive phase velocity of the surface (Rayleigh and/or Love) wave (Dorman and Ewing, 1962; Aki and Richards, 1980; Mari, 1984; Xia et al., 1999). For the case of a solid homogeneous half-space, the Rayleigh wave is not dispersive and travels with a velocity of approximately 0.9194v (Xia et al., 1999). Shear wave velocity profile was calculated using an iterative inversion process that requires the dispersion curve developed earlier as input. A least-squares approach allows automation of the process (Xia et al. 1999). S-wave velocities of each layer can be represented as the elements of a vector $\mathbf{x}$ of length n, or $\mathbf{x} = [v_{s1}, v_{s2}, v_{s3}, \ldots, v_{sn}]^T$. Similarly, the measurements (data) of Rayleigh-wave phase velocities at

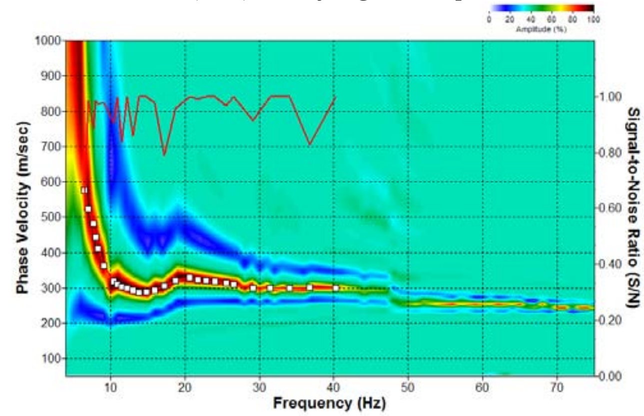

Fig. 3. Typical dispersion curve extracted from seismic data

m different frequencies can be represented as the elements of a vector $\mathbf{b}$ of length m, or $\mathbf{b}=[b_1, b_2, b_3, \ldots, b_m]^T$. Since the model $\mathbf{c}_R$ [equation (1)] is a nonlinear function, equation (1) must be linearized by Taylor-series expansion to employ the matrix theory:

$$J\Delta X = \Delta b \qquad (2)$$

where $\Delta\mathbf{b}=\mathbf{b}-\mathbf{c}_R(\mathbf{x}_0)$ and is the difference between measured data and model response to the initial estimation, in which $\mathbf{c}_R(\mathbf{x}_0)$ is the model response to the initial S-wave velocity estimates,$\mathbf{X}_0$; $\Delta\mathbf{X}$ is a modification of the initial estimation; and $\mathbf{J}$ is the Jacobian matrix with m rows and n columns ($m > n$). The elements of the Jacobian matrix are the first-order partial derivatives of $\mathbf{c}_R$ with respect to S-wave velocities. Since the number of data points contained in the dispersion curve is generally much larger than the number of layers used to define the subsurface ($m > n$), equation (2 is usually solved by optimization techniques. the objective function can be defined as

$$\Phi = \|J\Delta X - \Delta b\|_2 W \|J\Delta X - \Delta b\|_2 + \alpha\|\Delta X\|_2^2 \qquad (3)$$

where $\| \ \|_2$ is the l_2-norm length of a vector, α is the damping factor, and $\mathbf{W}$ is a weighting matrix. This is a constrained (weighted) least-squares problem. More details about the sensitivity of each parameter and calculation with respective examples are detailed in Xia et al., (1999). Shear wave velocities of each location were inverted from respective dispersion curves. The derived typical one-dimensional shear wave velocity (Vs) profile obtained using MASW is shown in Figure 4. These shear wave velocities of layers matches with drilled boreholes soil layers (Anbazhagan and Sitharam, 2009a).

STANDARD PENETRATION TEST N VALUES

The Standard Penetration Test (SPT) is one of the oldest, popular and most common in situ tests used for soil exploration in soil mechanics and foundation engineering. This test is being popularly used worldwide for many geotechnical projects, because of simplicity of the equipment and easiness of test procedure. In particular SPT test data are being used for seismic site characterization, site response and liquefaction studies towards seismic microzonation. This test is quite crude and depends on many factors, applications and equipment used in the test.

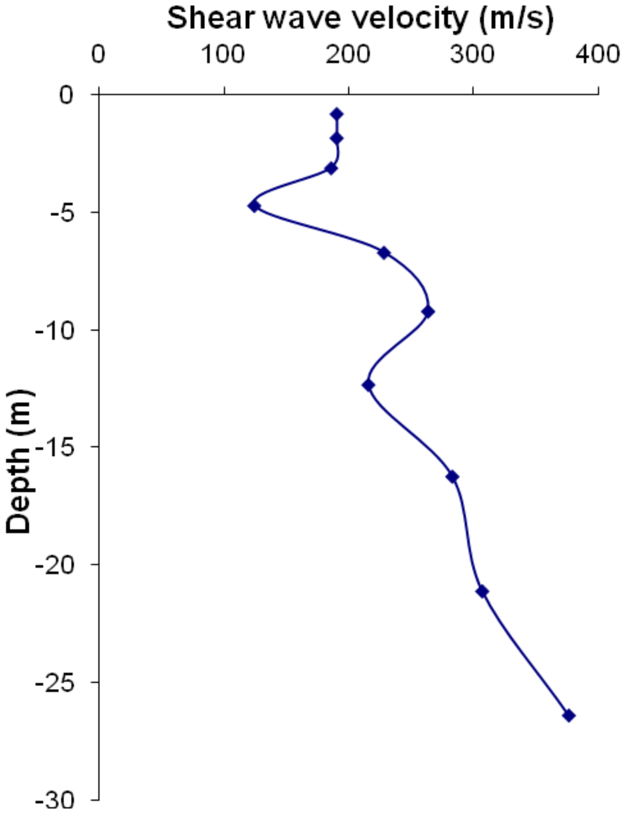

Fig.4. Typical shear wave velocity from MASW

The many factors includes drilling methods, drill rods, borehole sizes and stabilization, sampler, blow count rate, hammer configuration, energy corrections, fine content and test procedures (Schmertmann and Palacios, 1979; Kovacs et al., 1981; Farrar et al., 1998; Sivrikaya and Togrol, 2006). The combined effects of all of these factors can be accounted by applying the correction factors separately or together. The SPT N values may vary even for identical soil conditions because of sensitive to operating techniques, equipment, malfunctions and poor boring practice. So the SPT based correlations may be used for projects in preliminary stage or where there is a financial limitation, but for important projects it is preferable to measure dynamic properties directly by using field tests (Anbazhagan and Sitharam, 2008b).

Boreholes of 150mm diameter were drilled using hydraulic rotary drilling rigs up to the hard stratum at 38 locations. SPT tests were conducted at regular sampling interval of 1.5m in each borehole and additional disturbed soil samples were also collected. Most of the penetration resistances (SPT-N values) in boreholes are measured using donut hammer. The undisturbed soil samples were collected in the boreholes at possible depth by driving sampling tube of 100mm diameter and 300mm length. In-situ densities were evaluated from undisturbed soil samples. In most of the locations, the boreholes were drilled up to weathered rock and few locations up to hard rock. A typical borehole with SPT "N" values with depth is shown in Fig. 5.

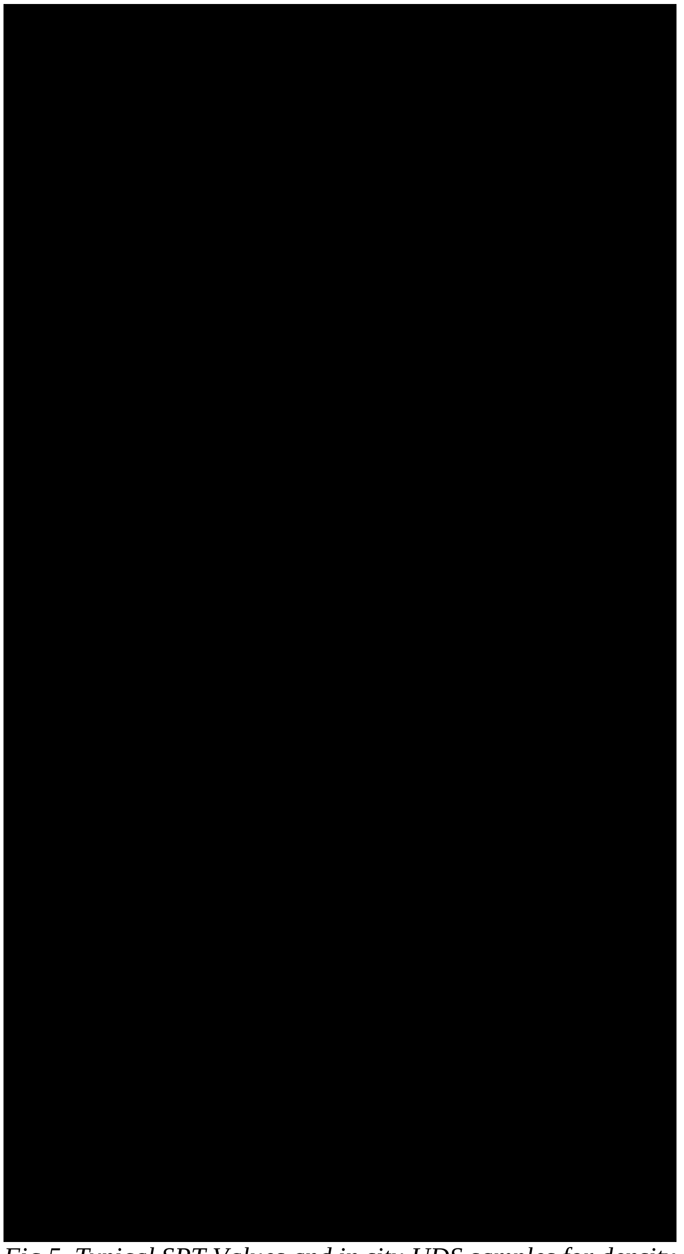

Fig.5. Typical SPT Values and in situ UDS samples for density

SPT N Corrections

The 'N' values measured in the field have been corrected for various corrections, such as: (a) Overburden Pressure (C_N), (b) Hammer energy (C_E), (c) Borehole diameter (C_B), (d) presence or absence of liner (C_S), (e) Rod length (C_R) and (f) fines content (C_{fines}) (Seed et al., 1983; 1985; Skempton, 1986; Youd et al., 2001; Cetin et al., 2004; Pearce and Baldwin, 2005). Corrected 'N' value i.e., $(N_1)_{60}$ are obtained using the following equation:

$$(N_1)_{60cs} = (N_1)_{60} + \Delta(N_1) \quad (4)$$

and $$(N_1)_{60} = N \times (C_N \times C_E \times C_B \times C_S \times C_R) \quad (5)$$

Where, $\Delta(N_1)$ is the correction factor for fines content. The values of correction factors, its upper limits and equation used were presented in Anbazhagan and Sitharam (2009b). Authors used SPT N values for estimation of ground response parameters and evaluated values are compared with field measurements. Shear wave velocity and boreholes considered in this study were also used for seismic Microzonation and liquefaction hazard mapping of Bangalore (Sitharam and Anbazhagan 2008a; Sitharam et al., 2007)

SHEAR MODULUS

The shear modulus at low strain level for soil layers has been determined using shear wave velocity from MASW and density from undistributed soil samples using equation (6):

$$G = \rho V_s^{\,2} = \gamma / g V_s^2 \quad (6)$$

Where, ρ is the density measured from the undisturbed sample, and, *Vs* is the shear wave velocity measured using the MASW testing. G_{max} has been evaluated for corresponding depth of N values in the respective locations. The correlation between measured G_{max} (calculated from measured shear wave velocity and density of each layer) to the measured SPT-N values is attempted. From the 38 locations, about 215 data pairs of *Vs* and G_{max} values have been used for the regression analysis. To obtain the practical relationship between shear modulus and N values and to understand data matching, different combinations of corrected and uncorrected values were attempted, as discussed below;

RELATION BETWEEN UNCORRECTED VALUES

Correlation between measured values of SPT- N and shear modulus (G_{max}) presented in Fig. 6 in log-log plot. The regression equation between G_{max} and N is given below:

$$G_{max} = 24.28 N^{0.55} \quad (7)$$

Where, G_{max} –Low strain measured shear modulus in MN/m^2, N – Measured SPT "N" Value. Figure 6 also shows the actual data and fitted equation with upper and lower bound. The best fit equation has the regression coefficient of R squared value of 0.88. In addition regression equations with 95% confidence interval are shown in Fig. 6. The 95% confidence bands enclose the area that one can be 95% sure of the true curve. It gives a visual sense of how well the data define the best-fit curve (Motulsky, 2008). Regression equations corresponding to 95% confidence intervals are given in equations 8 and 9, respectively.

Upper side on 95% confidence interval

$$G_{max} = 29.12 N^{0.60} \quad (8)$$

Lower side on 95% confidence interval

$$G_{max} = 19.43 N^{0.51} \quad (9)$$

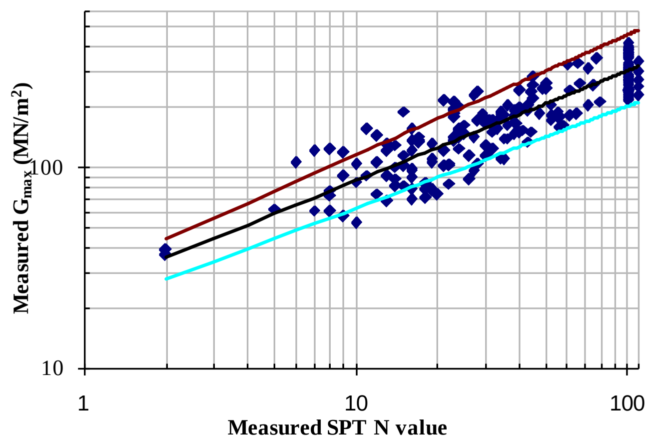

Fig. 7. Empirical correlation between measured shear modulus and SPT N values with upper and lower bound

RELATION BETWEEN CORRECTED N AND UNCORRECTED G_{MAX} VALUES

In order to study the difference between corrected and uncorrected SPT- N values in regression equation. The correlation between corrected N values and measured shear modulus are generated. The corrected N values are estimated excluding fine content correction factor according to equation 5 i.e $(N_1)_{60}$. Figure 8 shows the correlation between corrected N values and measured shear modulus. This relation gives R squared value of 0.860, which is lower than uncorrected correlation R squared value. The SPT corrected N values are in the range of 2 to about 90. The developed regression equation for the corrected N values without considering fines content correction is given below:

Without fines content correction

$$G_{max} = 29.17[(N_1)_{60}]^{0.57} \qquad (10)$$

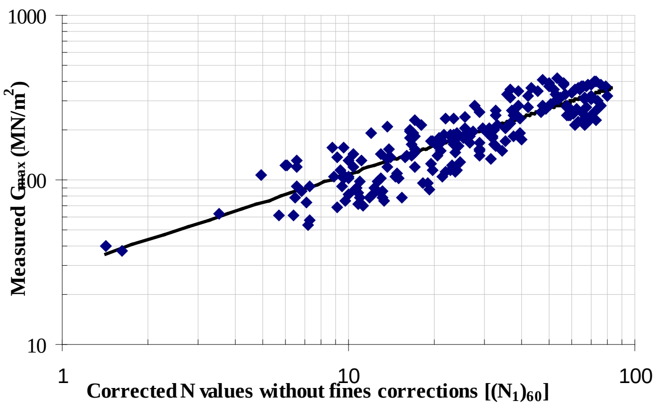

Fig. 8. Empirical correlation between measured shear modulus and corrected SPT N values without fines content correction

Next the correlation between corrected N values considering fines content corrections and measured shear modulus are generated. The corrected N values are estimated including fine content correction factor according to equation 4 i.e $(N_1)_{60cs}$. Figure 9 shows the correlation between corrected N values with fines content corrections and measured shear modulus. This relation gives R squared value of 0.858, which is slightly lower than previous R squared values. The developed regression equation for the corrected N values considering fines content correction is given below:

With fines content correction

$$G_{max} = 17.12\left[(N_1)_{60cs}\right]^{0.69} \qquad (11)$$

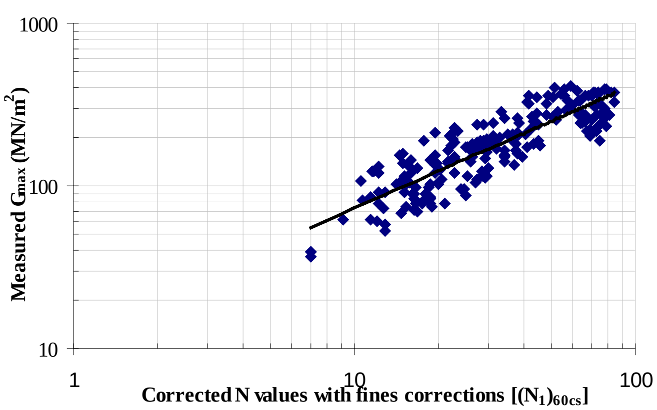

Fig. 9. Empirical correlation between measured shear modulus and corrected SPT N values with fines content correction

CORRELATION BETWEEN MEASURED AND CORRECTED N VALUES

SPT N values measured in field are more popular and are correlated with many soil properties. But the direct applications of the measured SPT N values in earthquake geotechnical engineering is limited. The measured SPT N values corrected for various corrections are as stated above. To compare the G_{max} regression equations developed in this study, measured N values and corrected N values $[(N_1)_{60}$ or $(N_1)_{60cs}]$ are related by simple regression equation. The best fit regression for the corrected N values without considering fines content correction $[(N_1)_{60}]$ and measured N values is shown in Fig. 10. The regression relation with R^2 value of 0.96 is given below:

$$(N_1)_{60} = 1.02(N)^{0.88} \qquad (12)$$

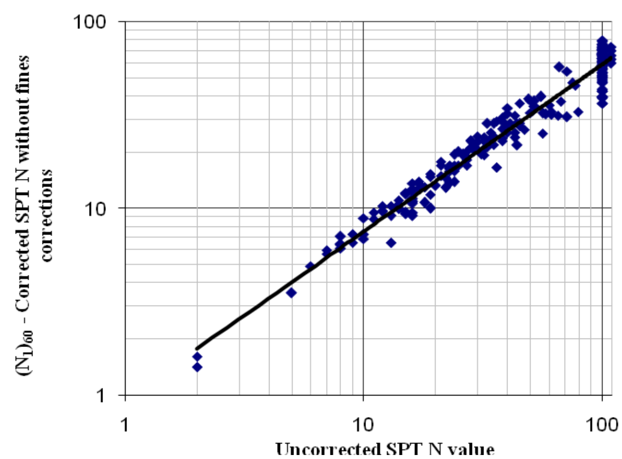

Fig. 10. Corrected N without fines content correction versus measured N values

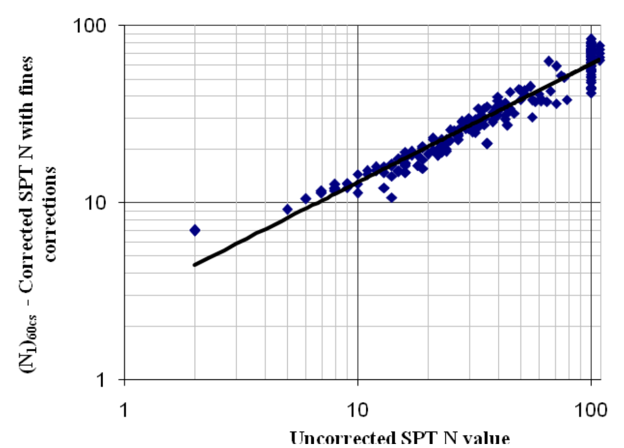

Fig. 11. Corrected N with fines content correction versus measured N values

Similarly the best fit regression for the corrected N values considering fines content correction [$(N_1)_{60cs}$] and measured N values is shown in Fig. 11. The regression relation with R^2 value of 0.96 is given below:

$$(N_1)_{60cs} = 2.17(N)^{0.74} \quad (13)$$

RESULTS AND DISCUSSIONS

G_{max} correlations developed in this study considering measured N values, corrected N values with and without considering fines content correction are plotted in Fig. 12. Figure 12 shows comparison of the equations 7, 10 and 11 using the above equations 12 and 13. In Figure 12, horizontal line (X axis) gives measured/ uncorrected or corrected SPT N values based on the equation considered. If SPT N value of X is uncorrected for equation 7, the same X is corrected N value without fines content correction for equation 10 and corrected N value with fines content correction for equation 11. Regression line for $(N_1)_{60}$ versus G_{max} is above the N versus G_{max} for all the N values. But the regression line for $(N_1)_{60cs}$ versus G_{max} is below the N versus G_{max} for the N values 8, coinciding for the N value of 8 to 20 and above for N value of beyond 20. Here it is interesting to note that regression relations $(N_1)_{60cs}$ versus G_{max} and N versus G_{max} are similar for N values ranging from 8 to 20 and G_{max} value of 60MPa to 150MPa. $(N_1)_{60}$ versus G_{max} and $(N_1)_{60cs}$ versus G_{max} are similar for N value of above 30.

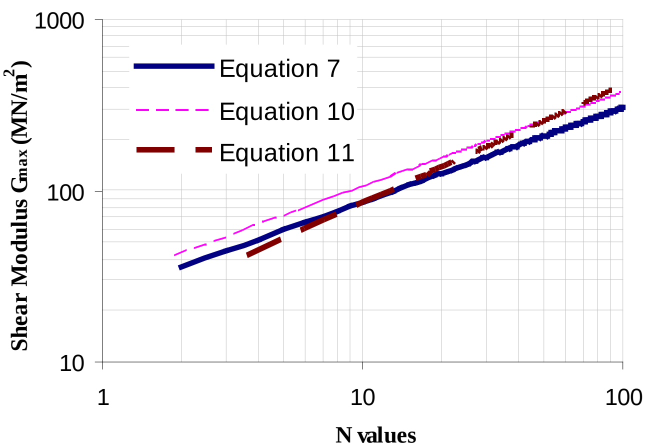

Figure 12: Comaprsion of correlation between measured and corrected N values.

SPT N versus G_{max} relation presented in this study has been compared with existing relations available in the very famous earthquake geotechnical engineering text books. The summary and compilation of relation between SPT N values and G_{max} was presented by Ishihara (1996). The author has plotted summary relations developed by others using straight line log-log plot and tabulated the constants of “a” and “b” for the below equation:

$$G_{max} = aN^b \quad (14)$$

The coefficient of “a” takes a value between 1.0 and 1.6 kPa and the exponent of N take a value of 0.6 to 0.8. Table 1 shows “a” and “b” for equations 14 presented in Ishihara (1996) and respective references.

Table 1: N versus G_{max} relations given in Ishihara (1996) table 6.4 page119.

Value of a (kPa)	Value of b	References
1	0.78	Imai and Yoshimura (1970)
1.22	0.62	Ohba and Toriumi (1970)
1.39	0.72	Ohta et al. (1972)
1.2	0.8	Ohsaki and Iwasaki (1973)
1.58	0.67	Hara et al. (1974)

This is the first text book which summarizes many SPT N versus shear modulus relations developed by others. In this book, the author has also highlighted that the SPT N value in Japanese practice is approximately 1.2 times smaller than the N_{60} values used in US practice (Ishihara, 1996). Seed et al., (1985) have given the summary of hammer energy ratio in SPT procedure followed in Japan, United States (US), Argentina and China and correction factor with respect to US. Figure 13 shows correlation presented by Ishihara, (1996) considering the Japanese SPT N values. It is a surprise to see that G_{max} values vary from 1.2 to 2.5kPa for SPT N value of 1 and 21 to 48 kPa for N value of 100. Another text book which has presented the summary of SPT N versus G_{max} is Kramer (1996). The equation similar to present study from Kramer (1996) is given below:

$$G_{max}(kips/ft^2) = 325[N_{60}]^{0.68} \quad (15)$$

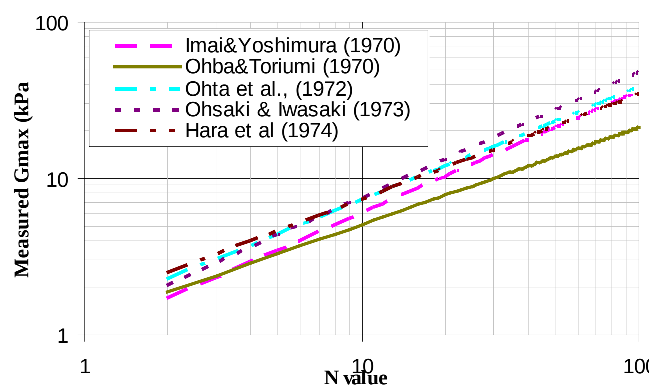

Figure 13: Plots of empirical correlation given in Ishihara (1996) Table 6.4, page 119.

Where N_{60} is the corrected SPT N value for hammer energy. This equation was valid only for sand and was reproduced from Imai and Tonouchi (1982) studies (Email communication with Kramer, 2009). According to Seed et al (1985) Japanese SPT N values were measured by applying hammer energy of 67 to 68 %, which is 1.12 to 1.3 times greater than US practice hammer energy of 60%. So Japanese SPT N values are corrected for 60% hammer energy (N_{60}). The N_{60} in the equation 15 corresponds to the 0.83 times measured N values considered by Imai and Tonouchi (1982). The equation 15 gives the G_{max} of 17663 kPa for the Japanese N value of 1 and 401882 kPa for Japanese N value of 100. This comparison clearly shows the N versus G_{max} relations given in Ishihara (1996), table 6.4, page119 gives very less G_{max} values when compared to Kramer (1996). This has been brought to notice to Ishihara by the first author and have requested clarification for the same (Email communication with Ishihara, on June 2009). Considering ambiguities in regression relation given in Ishihara (1996). The equations developed in this study are compared with the equation given in Kramer (1996), which is the reproduced equation from Imai and Tonouchi (1982). Imai and Tonouchi (1982) have developed N versus G_{max} relation using the average N values from single velocity layers. The SPT N values of above 50 and below 1 are substituted for the number of blows required to achieve a penetration depth of 30 cm from actual amount of penetration achieved at 50 blows. Figure 14 shows the Kramer (1996) equation considering Japanese N as well as N_{60}, along with data used in this study. The data used in this study is for sandy silt and silty sand with less clay content. Kramer's equations are applicable for sandy soil.

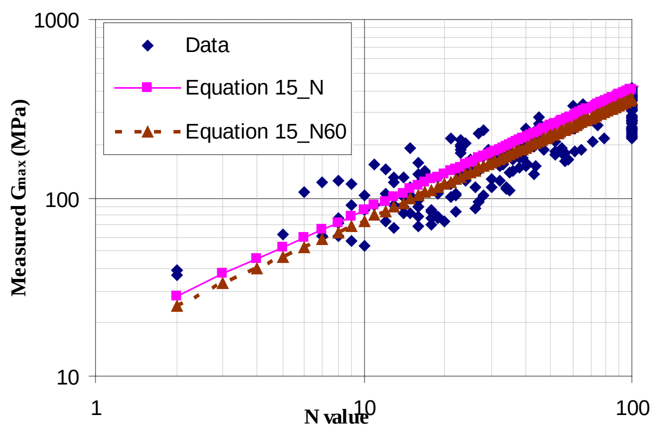

Figure 14: Our data with Kramer, (1996) referring Imai and Tonouchi, (1982) equation considering N and N_{60}

Figure 15 shows N versus G_{max} equation developed in this with upper and lower bound and Kramer (1996) equations. Kramer (1996) equations are in between upper and lower bound equations presented in this study. N versus G_{max} developed in this study is comparable with Kramer (1996) equation for measured values, but is not exactly coinciding with Kramer (1996) equation. This may be due to soil type and extrapolation involved in original equations presented by Imai and Tonouchi (1982). Further Kramer (1996) equations have been plotted with our G_{max} relations developed for measured and corrected N values. Figure 16 shows equations 7, 10 and 11 developed in this study with Kramer's equations for Japanese N with 10% error. Kramer (1996) equation for Japanese N values with 10% error matches with proposed regression equation of N versus G_{max} for the N value of 3 to 40. It also matches with proposed regression equation of $(N_1)_{60}$ versus G_{max} for the $(N_1)_{60}$ above 20. The proposed regression equation of $(N_1)_{60cs}$ versus G_{max} matches well with Kramer (1996) equation for all the N value. This may be attributed to fines content correction in $(N_1)_{60cs}$.

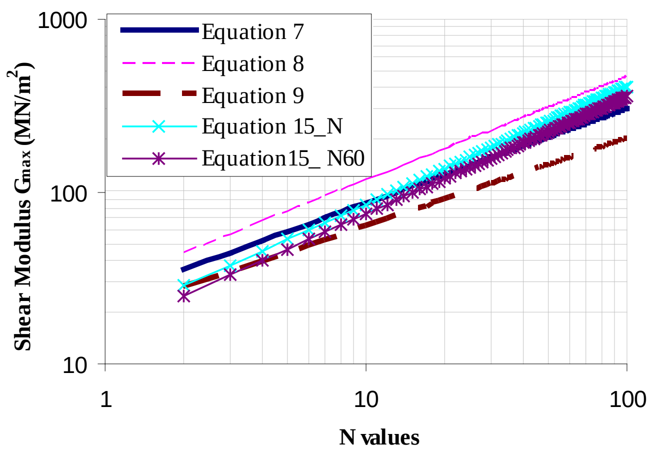

Figure 15: Proposed regression equation of N versus G_{max} with upper and lower bound and Kramer, (1996) referring Imai and Tonouchi, (1982) equation considering N and N_{60}

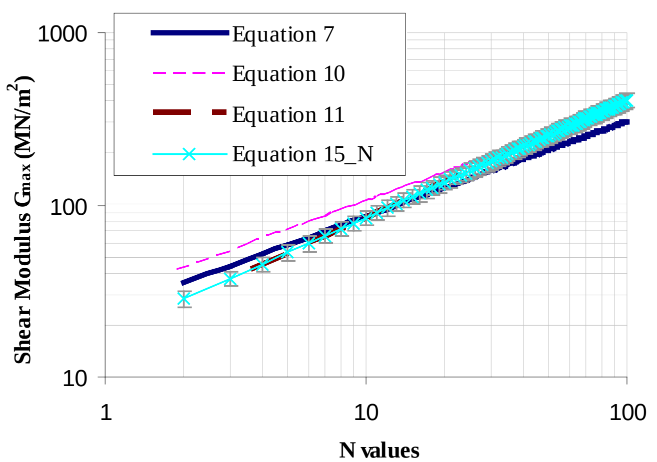

Figure 16: Proposed regression equations of N versus G_{max}, $(N_1)_{60}$ versus G_{max} and $(N_1)_{60cs}$ versus G_{max} with Kramer, (1996) referring Imai and Tonouchi, (1982) equation considering N

Figure 17 shows equations 7, 10 and 11 developed in this study with Kramer equations for N_{60} with 10% error. Kramer (1996) equation for N_{60} values with 10% error matches with proposed regression equation of N versus G_{max} and $(N_1)_{60cs}$ versus G_{max} for the N value of above 10. $(N_1)_{60}$ versus G_{max} is matches with Kramer (1996) equation for $(N_1)_{60}$ value beyond 50.

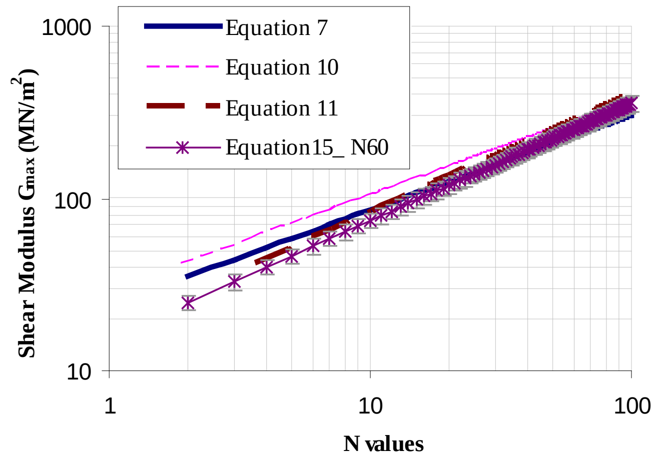

Figure 17: Proposed regression equations of N versus G_{max}, $(N_1)_{60}$ versus G_{max} and $(N_1)_{60cs}$ versus G_{max} with Kramer, (1996) referring Imai and Tonouchi, (1982) equation considering N_{60}

CONCLUSION

Regression relation between SPT N and G_{max} values has been developed using 215 pair of SPT N and G_{max} from geotechnical borelogs and geophysical MASW data. The regression equation using measured values gives best fit and more R squared values when compared to the corrected N and G_{max} relation. The regression relation between G_{max} and corrected N values without considering fines content correction $[(N_1)_{60}]$ or considering fines content correction $[(N_1)_{60cs}]$ also gives similar R squared values. Any one of the corrected N values (without or with considering fines content correction) can be used for regression analysis. The developed equation in study between N versus G_{max} is more suitable for residual soils (i.e silty sand or sandy silt) with less percentage of clay content. Regression relation developed in this study is compared with widely used equations available in literature for sandy soil. The proposed equation of $(N_1)_{60cs}$ versus G_{max} matches well with Kramer (1996) equation for Japanese N values and other two equations are comparable. Kramer's equations considering N_{60} is comparable with developed equations for N value of above 50. This may be attributed by corrections factors applied and soil type. The proposed equations are applicable for residual soils specifically sandy silt and silty sand with less clay content.

REFERENCES

Aki, K., and Richards, P. G. [1980]. "*Quantitative seismology*." W.H. Freeman & Co.

Anbazhagan P. and Sitharam, T. G. [2008b]. "Site Characterization and Site Response Studies Using Shear Wave Velocity", Journal of Seismology and Earthquake Engineering, Vol. 10(2), pp. 53-67.

Anbazhagan P., and Sitharam, T. G. [2009a]. "Spatial Variability of the Weathered and Engineering Bed rock using Multichannel Analysis of Surface Wave Survey". Pure and Applied Geophysics, Vol. 166, pp. 409–428.

Anbazhagan P., and Sitharam, T. G. [2009b]. "Estimation of Ground Response Parameters and comparison with field measurements", Indian Geotechnical Journal, Vol.39, No.3 pp. 245-270

Anbazhagan P., and Sitharam, T. G. [2010]. "Relationship between Low Strain Shear Modulus and Standard Penetration Test 'N' Values", Geotechnical Testing Journal, ASTM, GTJ102278-08R1 (under review).

Anbazhagan P., Sitharam, T. G. Vipin, K. S. [2009a]. "Site classification and estimation of surface level seismic hazard using geophysical data and probabilistic approach", Journal of Applied Geophysics, Vol. 68 (2), pp. 219-230.

Anbazhagan, P. and Sitharam, T. G. [2008a]. "Seismic Microzonation of Bangalore", Journal of Earth System Science, Vol.117(S2), pp. 833–852.

Anbazhagan, P., and Sitharam, T. G. [2008c]. "Mapping of Average Shear Wave Velocity for Bangalore Region: A Case Study," Journal of Environmental & Engineering Geophysics, Vol.13(2), pp. 69-84.

Anbazhagan, P., Indraratna, B., Rujikiatkamjorn, C., and Su, L. [2009b]. "Using a Seismic Survey to Measure the Shear Modulus of Clean and Fouled Ballast",. Geomechanics and Geoengineering: An International Journal - Manuscript ID TGEO-2009-0027 (Under consideration).

Cetin, K. O, Seed, R. B., Kiureghian, A. D., Tokimatsu, K., Harder, L. F. Jr., Kayen, R. E., and Moss, R. E. S. [2004]. "Standard penetration test-based probabilistic and deterministic assessment of seismic soil liquefaction potential", Journal of Geotechnical and Geoenvironmental Engineering, Vol. 12, pp 1314-1340.

Dorman, J., and Ewing, M. [1962] "Numerical inversion of seismic surface wave dispersion data and crust-mantle structure in the New York–Pennsylvania area," J. Geophys. Res., Vol.67,pp 5227–5241.

Farrar, J. A., Nickell, J., Alien, M. G., Goble, G. and Berger, J. [1998]. "Energy loss in long rod penetration testing — Terminus Dam liquefaction investigation." *Proceedings of the ASCE Specialty Conference on Geotechnical Earthquake Engineering and Soil Dynamics III, Seattle,* vol. 75, pp. 554–567.

Hara, A., Ohta, T., Niwa, M., Tanaka, S., and Banno, T. [1974]. "Shear modulus and shear strength of cohesive soils", Soils and Foundations, Vol.14, pp. 1-12.

Imai, T. and Yoshimura, Y. [1970]. “Elastic wave velocity and soil properties in soft soil (in Japanese)”. Tsuchito-Kiso Vol.18, No1, pp.17–22.

Imai, T., and Tonouchi, K., [1982]. “Correlation of N-value with S-wave velocity and shear modulus”, Proceedings, *2nd European Symposium on Penetration Testing, Amsterdam*, pp. 57-72.

Ishihara, K. [2009]. “*Soil dynamics; Earthquake engineering*” published by Clarendon Press, Oxford, New York.

Kanli, A. I., Tildy, P. Pronay, Z, Pinar, A., and Hemann, L. [2006]. “Vs30 mapping and soil classification for seismic site effect evaluation in Dinar region, SW Turkey”, Geophysics J. Int., Vol.165, pp.223-235.

Kovacs, W. D., Salomone, L. A. and Yokel, F. Y. [1981]. “*Energy Measurement in the Standard Penetration Test*”. U.S. Department of Commerce and National Bureau of Standards, Washington D.C.

Kramer, S. L. [1996]. “*Geotechnical Earthquake Engineering*,” Published by Pearson Education Ptd. Ltd, Reprinted 2003, Delhi, India.

Mari, J. L. [1984]. “Estimation of static correction for shear-wave profiling using the dispersion properties of Love waves”, Geophysics, Vol.49, pp.1169– 1179.

Miller, R. D. Xia, J. Park, C. B. and Ivanov, J. [1999]. “Multichannel analysis of surface waves to map bedrock,” The Leading Edge, Vol. 18, No.12, pp. 1392-1396.

Motulsky, H. [2008]. “Confidence and prediction bands, Graphing nonlinear regression,” *GraphPad Prism version 5.00 for Windows, GraphPad Software, San Diego California USA*, http://www.graphpad.com, last accessed on 23-08-2008.

Ohba, S. and Toriumi, I. [1970]. “Research on vibration characteristics of soil deposits in Osaka, part 2, on velocities of wave propagation and predominant periods of soil deposits”, *Abstract, Technical meeting of Architectural Institute of Japan (in Japanese)*.

Ohsaki, Y. and Iwasaki, R. [1973] “On dynamic shear moduli and Poisson’s ratio of soil deposits,”. Soil Found. Vol. 13, No.4, pp.61–73.

Park, C. B. Miller, R. D. and Xia, J. [1999]. “Multi-channel analysis of surface waves”, Geophysics, Vol. 64, No.3, pp. 800-808.

Park, C.B., Miller, R.D., and Miura, H. [2002]. “Optimum field parameters of an MASW survey [Exp. Abs.],” *SEG-J, Tokyo, May* , pp 22-23.

Pearce, J. T., and Baldwin, J. N. [2005]. “Liquefaction Susceptibility Mapping ST. Louis, Missouri and Illinois,”-*Final Technical Report, published in web.er.usgs.gov/reports/ abstract/2003/cu/03HQGR0029.pdf*.

Press, W. H., Teukosky, S. A., Vetterling, W. T., and Flannery, B. P. [1992]. “*Numerical recipes in C”*, Cambridge Univ. Press.

Schmertmann, J. H. and Palacios, A. [1979]. “Energy dynamics of SPT”. ASCE Journal of Geotechnical Engineering Division, Vol. 105, No.GT8, pp.909–926.

Schwab, F. A., and Knopoff, L. [1972]. “Fast surface wave and free mode computations,” *in Bolt,B. A., Ed., Methods in computational physics*: Academic Press, pp.87–180.

Seed, H. B., Idriss, I. M., and Arango, I. [1983]. “Evaluation of Liquefaction potential Using Field Performance Data,” Journal of Geotechnical Engineering, Vol. 109, No. 3, pp 458-482.

Seed, H. B., Tokimatsu, K., Harder, L. F., and Chung, R. M. [1985]. “The influence of SPT procedures in soil liquefaction resistance evaluations,” J. Geotech. Engg., ASCE, Vol.111, No.12, pp.1425–1445.

Sitharam, T. G. and Anbazhagan, P. [2008b]. “Evaluation of Low strain Dynamic properties using Geophysical method: A case study,” Consulting Ahead, Vol.2, No.2, pp. 34-50.

Sitharam, T. G., Anbazhagan. P. and Mahesh. G. U. [2007]. “3-D Subsurface Modelling and Preliminary Liquefaction Hazard Mapping of Bangalore City Using SPT Data and GIS”, Indian Geotechnical Journal, Vol.37, No.3, pp. 210-226.

Sitharam, T.G. and Anbazhagan, P. [2008a]. “Seismic Microzonation: Principles, Practices and Experiments,” EJGE Special Volume Bouquet 08, online, http://www.ejge.com/Bouquet08/Preface.htm, P-61.

Sivrikaya, O. and Toğrol, E. [2006]. “Determination of undrained strength of fine-grained soils by means of SPT and its application in Turkey”. Engineering Geology, Vol. 86, pp. 52–69.

Skempton, A. W. [1986]. “Standard Penetration Test Procedures,” Geotechnique, Vol.36, No.3, pp 425-447.

Xia, J., Miller, R.D., and Park, C.B., [1999]. “Estimation of near-surface shear-wave velocity by inversion of Rayleigh wave,” Geophysics, Vol.64, No.3, pp. 691-700.

Youd, T.L., Idriss, I.M., Andrus, R.D., Arango, I., Castro, G., Christian, J.T., Dobry, R., Liam Finn, W.D., Harder Jr., L.H., Hynes, M.E., Ishihara, K., Koester, J.P., Liao, S.S.C, Marcuson, W.F., Marting, G.R., Mitchell, J.K., Moriwaki, Y., Power, M.S., Robertson, P.K., Seed, R.B, And Stokoe, K.H., [2001]. “Liquefaction Resistance of Soils: Summary from the 1996 NCEER and 1998. NCEER/NSF Workshops on Evaluation of Liquefaction Resistance of Soils,” Journal of Geotechnical and Geoenvironmental Engineering, pp 817 – 833.